Journal of the Brazilian Society of Mechanical Sciences and Engineering (2020) 42:605
https://doi.org/10.1007/s40430-020-02681-z

TECHNICAL PAPER

Rheological modeling of multi-phase shear thickening fluid using an intelligent methodology

Selim Gürgen[1] · Mehmet Alper Sofuoğlu[2] · Melih Cemal Kuşhan[2]

Received: 10 February 2020 / Accepted: 10 October 2020
© The Brazilian Society of Mechanical Sciences and Engineering 2020

Abstract
Shear thickening fluid (STF) has been extensively utilized in various engineering applications due to its unique characteristic, which is increasing viscosity under loading. Although single-phase STF is known for a long time, STF has been introduced to a novel concept, namely multi-phase STF, which includes particle additives in the suspension. In the STF adaptation to different systems, STF rheology is the key factor that should be tuned precisely for efficient usage. For this reason, STF rheology has been investigated by many researchers; however, experimental measurements are highly tedious and time-consuming. At this stage, theoretical modeling emerges as a wise choice; however, these models lead to a heavy computational burden due to the complex STF rheology. Therefore, we benefited from an intelligent modeling methodology that is highly effective for modeling and optimizing the complex and nonlinear relationships as such in multi-phase STF rheology. In this study, the rheology of multi-phase STF is investigated for the first time using an intelligent model to the best of our knowledge. According to the results, intelligent modeling is very efficient due to its parameter-free algorithm and successful fitting capability.

Keywords Shear thickening fluid · Silicon carbide · Rheology · Intelligent modeling

1 Introduction

Shear thickening fluid (STF) is a suspension having increasing viscosity under applied loading. This smart fluid consists of nano-sized colloidal particles responsible for the viscosity jump, in a liquid medium [1, 2]. Shear thickening behavior is explained by hydro-clustering theory, which suggests that hydrodynamic forces acting on the colloidal particles increase under elevated shear rates. Therefore, the particles form small groups, namely hydro-clusters in the suspension. At further shear rates, the colloidal particles come closer and physical contacts are observed as well as extending the hydro-clusters in the flow medium. The jump in the viscosity stems from the elongated particle clusters, which behave as obstacles and thereby stopping the fluid from flowing [3]. A recent approach, namely contact rheology model, supports the hydro-clustering theory in such a way that hydrodynamic interaction is responsible for the shear thickening onset at lower shear rates; however, at higher shear rates, the contribution of particle contacts within the hydro-clusters is much higher than the hydrodynamic interaction to the shear thickening mechanism [4, 5]. STF rheology has been investigated by many researchers on the one hand [6–11]; STF has been adapted to different kinds of engineering applications on the other [12–17]. Since STF has been efficiently utilized in vibration damping systems [18–20], polishing processes [21, 22] and protective structures [23, 24], STF rheology should be understood in detail to adjust the systems as requested. For this reason, researchers developed different theoretical models to predict the STF rheology. Galindo-Rosales et al. [25] proposed a phenomenological model based on a broad set of experimental data. In their other work [26], a small modification was done in their model to make the fitting parameters more natural. However, the model divides a typical STF flow curve into 3 main regions since complex flow characteristics cannot be fitted in one attempt. Hence, this model requires 11 independent parameters which must be obtained from experimental measurements before the iterative fitting procedure. Although the accuracy of this

Technical Editor:Edson José Soares.

✉ Mehmet Alper Sofuoğlu
asofuoglu@ogu.edu.tr

[1] Eskişehir Vocational School, ESOGU, 26110 Eskişehir, Turkey

[2] Department of Mechanical Engineering, ESOGU, 26480 Eskişehir, Turkey

Published online: 29 October 2020

model is highly sufficient, there is a significant computational expense that makes the model complicated. Tian et al. [27] extended Galindo-Rosales et al. [25]'s model to predict the rheology of STF at different temperatures. However, a number of rheological measurements at various temperatures were performed as well as determining the parameters in the viscosity functions. In order to eliminate the time-consuming calculations, Wei et al. [28] developed a simple phenomenological model to predict the rheology of STF; however, they assumed that STF exhibits Newtonian behavior until the thickening point. Although this assumption is mostly valid for single-phase STF systems, it fails in the multi-phase suspensions since the viscosity curve of multi-phase STF shows considerable shear-thinning until the thickening onset. For this reason, we proposed a modified model based on Wei et al. [28]'s work in a recent study [29] and thereby fully capturing the flow characteristics of the multi-phase STF, including the pre-thickening region. It was the first study considering the modeling of multi-phase STF and now, we have developed another model for the multi-phase system by taking advantage of one of an intelligent methodology; artificial neural networks (ANN) for the first time in literature. Since ANN method is highly effective for modeling and optimizing complex and non-linear relationships, multi-phase STF rheology is a proper problem in full measure for this intelligent method. Arora et al. [7] benefited from intelligent modeling for the prediction of STF rheology, but they investigated single-phase systems. According to their study, single-phase rheology is successfully captured by this parameter-free model. Since multi-phase STF rheology is more complicated than single-phase one, intelligent modeling methods are much more necessary for multi-phase systems where theoretical modeling requires a heavy computational burden and time-consuming process to the researchers. From this point of view, in the present work, we have developed an ANN modeling using a broad set of rheological data for multi-phase STF. The investigated STF was fabricated by mixing nano-sized silica particles in polyethylene glycol, and 3 different particle sizes of silicon carbides were included in the suspensions as an additive phase. The additive amount and temperature were also varied in the investigations. According to the results, ANN modeling gives successful fitting to the multi-phase rheology; however, at excessive additive amounts, model efficiency has a loss of performance due to the disruption of shear thickening behavior.

2 Experimental details

In this study, nano-sized silica with a particle size of 20 nm was supplied from Evonik. The silica particles were distributed in a polyethylene glycol (PEG) with a molar mass of 400 g/mol to fabricate single-phase STF. The silica concentration was 20 wt%, which is the maximum amount to avoid the bulky behavior of suspension. In order to prepare multi-phase systems, 3 different sizes of silicon carbide (SiC) particles, which were supplied from H.C. Starck Group, were included in this suspension. Figure 1 shows the scanning electron microscope image and particle size distribution of the SiC particles. Three different SiC concentrations (5, 25 and 45 wt%) were used in the suspensions based upon the overall STF weight. In the suspension preparation stage, a high-speed homogenizer was utilized for 40 min. In the rheological measurements, a MCR 301 Anton Paar stress-controlled rheometer was utilized with a temperature control device. The gap between the parallel plates was kept at 0.20 mm, and the tests were carried out within the shear rate of 0–1000 s^{-1}. The suspensions were tested at 3 different temperatures, which were controlled by the temperature control system connected to the bottom plate of the rheometer. A full factorial design was employed, and therefore, 27 measurements were performed in the rheological tests.

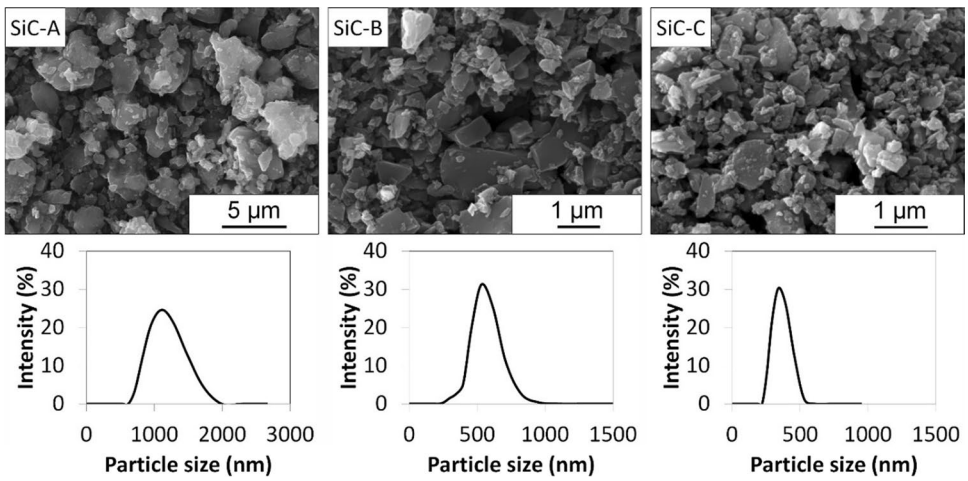


Fig. 1 Scanning electron microscope image and particles size distribution of the SiC particles

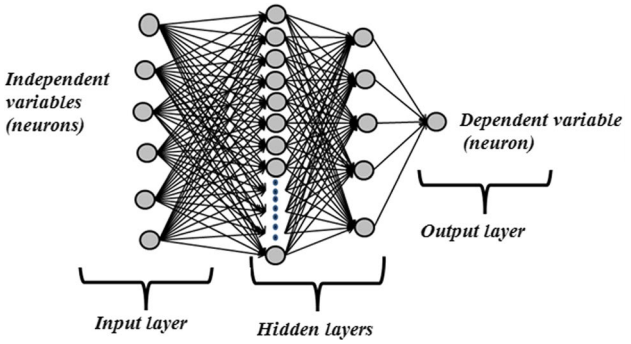


Fig. 2 An example of an ANN topology

Table 1 Variables in the rheological measurements

Parameter level	Additive particle size (μm)	Additive amount (wt%)	Temperature(°C)
1	1.114 (SiC-A)	5	20
2	0.512 (SiC-B)	25	40
3	0.340 (SiC-C)	45	60

Table 1 gives the variables and their levels in the rheological measurements (Fig. 2).

3 Artificial neural network (ANN) modeling

Artificial neural network (ANN) is a computing system formed by a plurality of simple processing units connected in some way. It possesses functions of learning, memory, association and calculation and can simulate the structure and function of the human brain's neural networks. By adaptive information processing, ANN can effectively deal with data with model uncertainty [30, 31]. An ANN topology is given in Figure 2.

The viscosity curves of multi-phase shear thickening fluids are predicted by the ANN method in the present work. In the modeling, the viscosity was dependent on 4 variables, such as additive particle size, additive amount, temperature and shear rate. A data-mining program, SPSS Clementine 10.1, was used for the ANN analyses. Three different training algorithms, namely Quick, Dynamic and Multiple, were employed to determine the importance level of the variables. The Quick algorithm uses certain rules and data characteristics to choose an appropriate topology for the network. The Dynamic algorithm creates an initial topology for the network and improves the topology by adding and/or removing hidden units as training progresses. The Multiple algorithm creates several neural networks of different topologies initially, and at the end of the training, the model with the lowest root means square error (RMSE) is selected as the final model. The Multiple algorithm is more comprehensive in comparison with the other ones, whereas the Dynamic algorithm conducts an extensive search with respect to the Quick algorithm. The Dynamic and Multiple algorithms change the network, but the Quick algorithm does not. These networks are trained using a parallel method. The ANN parameters used in the prediction models are provided in Table 2. The best network topology was obtained by an accuracy rate within the specified period. The training algorithms were used for the entire data set, and partial weights of the variables were found, which are given in Table 3. After different trials, 75/25 (%) training/testing ratio was selected for the models since this ratio produces successful results. According to the selected training/testing ratio, 900 data were used for training, whereas 300 data were used for testing.

Table 2 Model parameters

Parameters	Values and descriptions
Accuracy rate as a stopping criterion	100%
Analysis time	300 s
Network choice	Best result one selected
Initial weights	Randomly selected

Table 3 Partial weights for the training algorithms

Variables	Training algorithms		
	Quick	Dynamic	Multiple
Shear rate	0.17	0.14	0.15
Temperature	0.17	0.17	0.17
Additive ratio	0.09	0.12	0.12
Particle size	0.05	0.02	0.02

In the training algorithms, 4 neurons were used in the input layer to predict the suspension viscosity. One neuron was used in the output layer and a different number of hidden layers were used depending on the algorithms. In the Quick algorithm, 1 hidden layer with 3 neurons was used. In the Dynamic algorithm, 2 hidden layers with 28 and 12 neurons were used. In the Multiple algorithm, 2 hidden layers with 7 and 5 neurons were used. The hidden layers, the number of neurons and model parameters were determined by the algorithm based on the lowest RMSE values. From the results, it was seen that the Multiple training algorithm is the most appropriate algorithm for the viscosity prediction. In this algorithm, the determination coefficient (R^2) was 0.87 and 0.80 for the training and testing stages, respectively. Furthermore, the RMSE values were quite low such as 7.97 for the training stage and 9.15 for the testing stage.

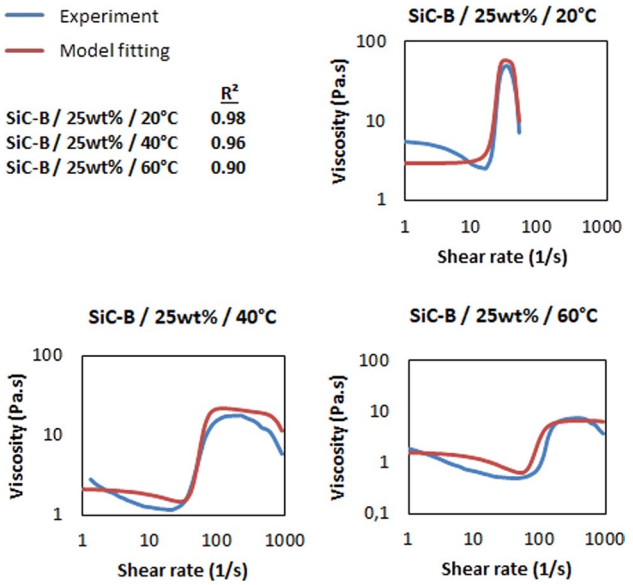


Fig. 3 Rheological curves for different temperatures in the training stage

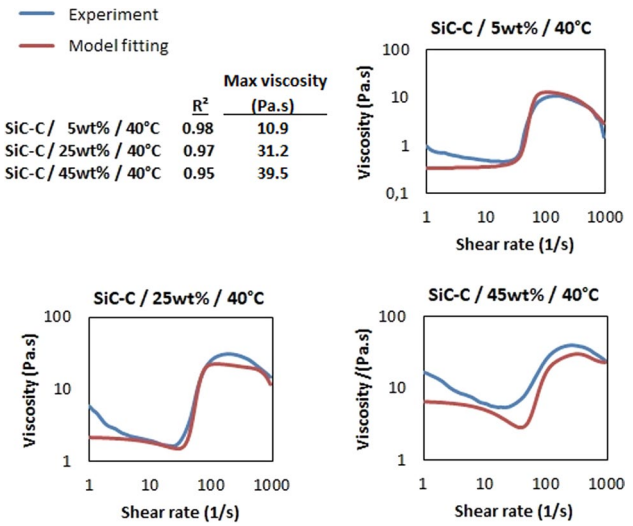


Fig. 4 Rheological curves for different amounts of additives in the training stage

4 Results and discussion

Figure 3 and 4 show the experimental and model fitting curves for different temperatures and additive amounts in the training stage. Considering the experimental results, the rheological curves exhibit a typical STF behavior under increasing shear rate. Until a critical point, the initial viscosity of the suspension slightly reduces as the shear rate increases. During this period, the suspension shows a shear-thinning behavior because, at zero shear point, the silica particles within the suspension establish weak physical bonds each other and by breaking these bonds due the increased shear rate, the silica particles form a layered orientation which provides a self-lubricating effect and consequently facilitating the flowability by reducing the viscosity. At the elevated shear rates, the hydrodynamic forces acting on the particles grow up and therefore, dense silica particle groups are formed in the suspension. These particle units are called hydro-clusters, and they hinder the suspension from flowing by playing the role of obstacles. As the shear rate further increases, silica particles physically touch each other and thus, hydro-clusters are extended within the suspension. By developing these particle structures, the suspension viscosity drastically jumps to a peak level. At the peak point, the elongated hydro-clustering network is broken and subsequently, the viscosity reduces. Considering the maximum viscosities in Fig. 4, there is an increasing trend by adding more carbide particles in the mixtures. This change is attributed to the increased solid content, which results in denser suspensions by the effect of an additional solid phase [1, 32]. From the point of view of the ANN modeling, each fitting curve represents this typical STF behavior. However, the fitting curves are better in covering the shear thickening regions rather than the shear thinning behavior at lower shear rates. Since the main characteristic of STF is the viscosity jump beyond the critical shear rate, it is possible to mention that the model is efficient in giving this behavior despite some deviations in the shear-thinning regions. According to the fitting curves, it can be stated that the ANN model is efficient in capturing the nonlinear relationships between the parameters. In addition to the overall trend in the curves, the correlation factors (R^2) for each case show very high values, which means that the model fitting is highly sufficient.

Fitting efficiency of the model is discussed in terms of RMSE and R^2 values, which are widely preferred to measure the differences between the predicted and observed values. RMSE gives the deviation amount in the fitting results, whereas R^2 shows the performance of the curve trend with respect to the experimental data. Therefore, in the evaluation of the results, both parameters should be taken into account for a proper assessment. Figure 5 and 6 show these performance parameters for the suspensions in the training stage. From the results, RMSE values exhibit very low values within the range of 0.52–10.37, which means that error in the model fitting is quite low; however, the suspensions, including 45wt% carbides at 20 °C, violate this lower trend in RMSE. This conflict may arise from the inclusion of the SiC additives, which disrupt the shear thickening behavior in the suspensions. As discussed in early works [32, 33], interstitial SiC particles in the silica clusters divide the silica groups into small units. For this reason, the interaction

between the nano-sized silica particles is interrupted by micron-sized carbides and therefore, hydro-clustering is hindered from extending in the suspension on a large scale and consequently, shear thickening is suppressed. As suggested in a previous work [3], hydrodynamic stresses are related to the cube of the cluster's larger dimension which proves that extended silica clusters are more beneficial than divided clusters to the shear thickening mechanism because shear thickening grows up when contacted microstructure is elongated by covering the medium as a force network in the suspension. From this point of view, at higher additive concentrations such as 45 wt%, shear thickening behavior fades away and therefore, the model fitting has a loss of performance as seen in the RMSE values. On the other hand, R^2 values exhibit higher rates; above 0.80, which means that the trend of the rheological curves is mostly captured by the model. There is no obvious systematic variation in the R^2 values depending on the parameters. This can be attributed to high level of R^2 values, which are close to each other in a narrow band.

Figure 7 shows the performance parameters of RMSE and R^2 for the suspensions in the testing stage. In this stage, the model yields insufficient fitting for the suspensions with 45wt% additive amount and therefore, these suspensions are excluded in the results. In fact, the main reason for poor fitting in the 45 wt% SiC suspensions is disrupted

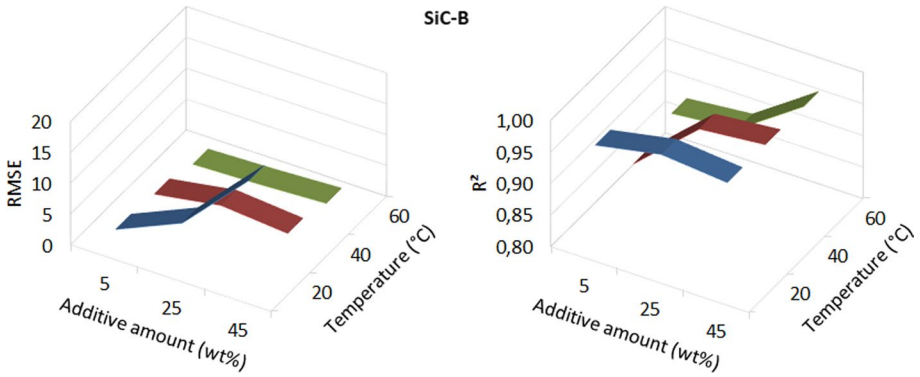


Fig. 5 Performance parameters for the suspensions including additive SiC-B in the training stage

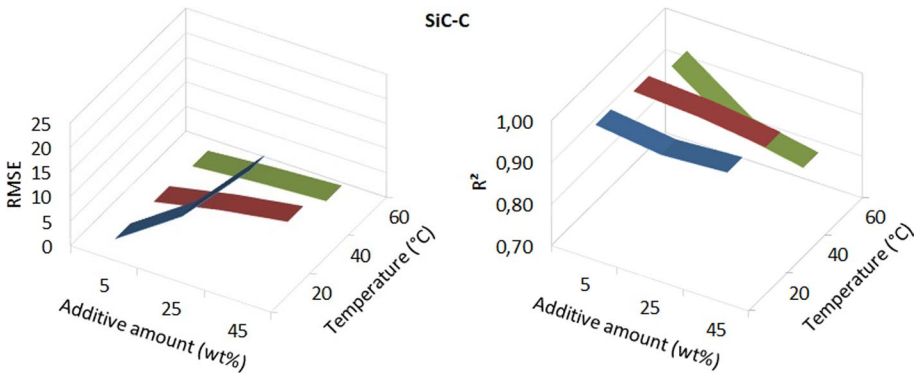


Fig. 6 Performance parameters for the suspensions including additive SiC-C in the training stage

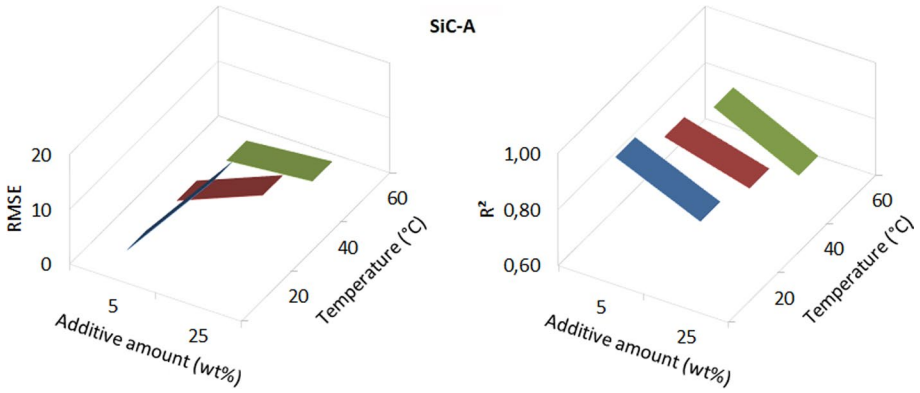


Fig. 7 Performance parameters for the suspensions including additive SiC-A in the testing stage

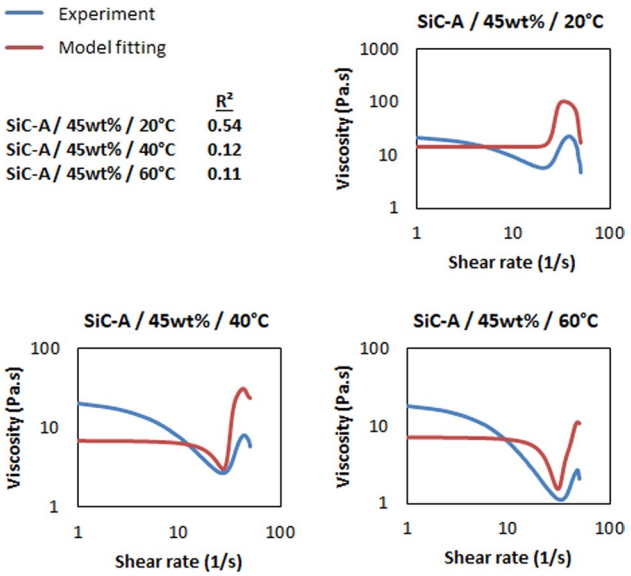


Fig. 8 Rheological curves for 45 wt% additives in the testing stage

shear thickening behavior. Figure 8 shows the rheological curves for these suspensions. Considering the experimental flow curves, the viscosity jump is very weak, which means that the peak viscosity beyond the thickening point is lower than the initial viscosity for each suspension. This is due to the excessive amount of SiC additives, which results in an attenuated shear thickening by breaking the extension of the hydro-clusters as well as increasing the initial viscosity of the mixtures. The inclusion of additives makes the mixtures denser due to the increased concentration of the solid phase. Hence, weak physical bonding at zero shear rate grows stronger due to closer particles that apply higher attractive forces to each other. For this reason, overall viscosity is enhanced in dense suspensions; however, the elongation of the silica clusters is restrained by these SiC particles. As a result of this process, the suspensions, including 45 wt% SiC particles do not exhibit a typical STF rheology and therefore, the developed model cannot predict the disrupted flow curves. On the other hand, at lower additive amounts, the suspensions keep shear thickening characteristics and thus, the model can efficiently capture the suspension flow curves. From the performance charts in Fig. 7, the RMSE results exhibit a similar trend with those in the training stage that error in the fittings increases by adding more carbides into the suspensions, especially at 20 °C. Although this increasing trend is also valid at higher temperatures, the change in RMSE is much slighter at 40 °C and 60 °C. At this juncture, it is better to discuss the temperature effect on the shear thickening behavior. Recalling Fig. 3, elevated temperature leads to a thinning effect on the overall viscosity, which is clearly seen from the initial viscosities; 5.47 Pa.s at 20 °C, 1.56 Pa.s at 40 °C and 1.32 Pa.s at 60 °C. This viscosity reduction is simply due to the weakening of the inter-particle adhesion forces triggered by the enhanced particle energy with the temperature rise [34, 35]. Although overall viscosity is affected by temperature, shear thickening mechanism is not disrupted heavily, at least, the suspensions sustain the shear thickening behavior by considering the experimental flow curves. Thus, the model fitting is quite efficient for the suspensions having additive amounts lower than 45 wt% at each temperature level.

5 Conclusions

In the present work, the rheological behavior of multi-phase STFs having different additive size and amounts at various temperatures was investigated using ANN modeling. RMSE and R^2 values, which represent the performance of the model fitting, were considered in the evaluation of the modeling. According to the results, the proposed model yields efficient fitting for the multi-phase STF systems since the rheological curves can be mostly captured by the developed model, however, at excessive additive loadings such as 45 wt%, the model has a loss of performance due to the disruption in the shear thickening behavior. Considering that multi-phase STFs are complex systems having non-Newtonian behavior, rheological prediction of these suspensions is highly tedious by theoretical models since they require several parameters for computing. Contrary to the computational burden in the theoretical models, ANN is a parameter-free model, which generates a mapping based on the relationship between the experimental inputs and outputs. Since these smart fluids have been adapted to various engineering applications such as vibration damping systems, polishing operations and protective structures, their rheologies should be predicted easily instead of conducting time-consuming experiments.

Compliance with ethical standards

Conflict of interest The authors declare that they have no competing interest.

Ethical approval This article does not contain any studies with human participants or animals performed by any of the authors.

References

1. Gürgen S, Kuşhan MC, Li W (2017) Shear thickening fluids in protective applications: a review. ProgPolymSci 75:48–72. https://doi.org/10.1016/j.progpolymsci.2017.07.003
2. Gürgen S (2019a) Tuning the rheology of nano-sized silica suspensions with silicon nitride particles. J Nano Res 56:63–70. https://doi.org/10.4028/www.scientific.net/JNanoR.56.63

3. Bossis G, Brady JF (1989) The rheology of Brownian suspensions. J ChemPhys 91(3):1866–1874. https://doi.org/10.1063/1.457091
4. Lin NYC et al (2015) Hydrodynamic and Contact Contributions to Continuous Shear Thickening in Colloidal Suspensions. Phys Rev Lett 115(22):228304. https://doi.org/10.1103/PhysRevLett.115.228304
5. Peters IR, Majumdar S, Jaeger HM (2016) Direct observation of dynamic shear jamming in dense suspensions. Nature 532(7598):214–217. https://doi.org/10.1038/nature17167
6. Gürgen S, Kuşhan MC (2016) Rheological properties of shear thickening fluids. J Polytech. 19(4):409–414
7. Arora S, Laha A, Majumdar A, Butola BS (2017) Prediction of rheology of shear thickening fluids using phenomenological and artificial neural network models. Korea-AustRheol J 29(3):185–193. https://doi.org/10.1007/s13367-017-0019-x
8. Zhang XZ, Li WH, Gong XL (2008) The rheology of shear thickening fluid (STF) and the dynamic performance of an STF-filled damper. Smart Mater Struct 17(3):035027. https://doi.org/10.1088/0964-1726/17/3/035027
9. Ghosh A, Chauhan I, Majumdar A, Butola BS (2017) Influence of cellulose nanofibers on the rheological behavior of silica-based shear-thickening fluid. Cellulose 24(10):4163–4171. https://doi.org/10.1007/s10570-017-1440-5
10. Moriana AD, Tian T, Sencadas V, Li W (2016) Comparison of rheological behaviors with fumed silica-based shear thickening fluids. Korea-AustRheol J 28(3):197–205. https://doi.org/10.1007/s13367-016-0020-9
11. Li S, Wang J, Zhao S, Cai W, Wang Z, Wang S (2017) Giant rheological effect of shear thickening suspension comprising silica nanoparticles with no aggregation. J Mater SciTechnol 33(3):261–265. https://doi.org/10.1016/j.jmst.2016.06.008
12. Fischer C, Braun SA, Bourban P-E, Michaud V, Plummer CJG, Månson J-AE (2006) Dynamic properties of sandwich structures with integrated shear-thickening fluids. Smart Mater Struct 15(5):1467–1475. https://doi.org/10.1088/0964-1726/15/5/036
13. Majumdar A, Butola BS, Srivastava A (2014) Development of soft composite materials with improved impact resistance using Kevlar fabric and nano-silica based shear thickening fluid. Mater Des 1980–2015 54:295–300
14. Gürgen S, Kuşhan MC (2017a) The stab resistance of fabrics impregnated with shear thickening fluids including various particle size of additives. Compos Part ApplSciManuf 94:50–60. https://doi.org/10.1016/j.compositesa.2016.12.019
15. Gürgen S, Kuşhan MC (2017b) The ballistic performance of aramid based fabrics impregnated with multi-phase shear thickening fluids. Polym Test 64:296–306. https://doi.org/10.1016/j.polymertesting.2017.11.003
16. Gürgen S, Kuşhan MC (2017c) The effect of silicon carbide additives on the stab resistance of shear thickening fluid treated fabrics. MechAdv Mater Struct 24(16):1381–1390. https://doi.org/10.1080/15376494.2016.1231355
17. Li M, Lyu B, Yuan J, Dong C, Dai W (2015) Shear-thickening polishing method. Int J Mach Tools Manuf 94:88–99. https://doi.org/10.1016/j.ijmachtools.2015.04.010
18. Gürgen S, Sofuoğlu MA (2019) Experimental investigation on vibration characteristics of shear thickening fluid filled CFRP tubes. Compos Struct 226:111236. https://doi.org/10.1016/j.compstruct.2019.111236
19. Gürgen S, Sofuoğlu MA (2020a) Vibration attenuation of sandwich structures filled with shear thickening fluids. Compos Part B Eng 186:107831. https://doi.org/10.1016/j.compositesb.2020.107831
20. Gürgen S, Sofuoğlu MA (2020b) Integration of shear thickening fluid into cutting tools for improved turning operations. J Manuf Process 56:1146–1154. https://doi.org/10.1016/j.jmapro.2020.06.012
21. Nguyen D-N et al (2020) Machining parameter optimization in shear thickening polishing of gear surfaces. J Mater Res Technol 9(3):5112–5126. https://doi.org/10.1016/j.jmrt.2020.03.028
22. Gürgen S, Sert A (2019) Polishing operation of a steel bar in a shear thickening fluid medium. Compos Part B Eng 175:107127. https://doi.org/10.1016/j.compositesb.2019.107127
23. Gürgen S (2019b) An investigation on composite laminates including shear thickening fluid under stab condition. J Compos Mater 53(8):1111–1122. https://doi.org/10.1177/0021998318796158
24. Gürgen S, Yıldız T (2020) Stab resistance of smart polymer coated textiles reinforced with particle additives. Compos Struct 235:111812. https://doi.org/10.1016/j.compstruct.2019.111812
25. Galindo-Rosales FJ, Rubio-Hernández FJ, Sevilla A (2011) An apparent viscosity function for shear thickening fluids. J Non-Newton Fluid Mech 166(5–6):321–325. https://doi.org/10.1016/j.jnnfm.2011.01.001
26. Galindo-Rosales FJ, Rubio-Hernández FJ, Sevilla A, Ewoldt RH (2011) How Dr. Malcom M. Cross may have tackled the development of 'an apparent viscosity function for shear thickening fluids.' J Non-Newton Fluid Mech 166(23–24):1421–1424. https://doi.org/10.1016/j.jnnfm.2011.08.008
27. Tian T, Peng G, Li W, Ding J, Nakano M (2015) Experimental and modelling study of the effect of temperature on shear thickening fluids. Korea-AustRheol J 27(1):17–24. https://doi.org/10.1007/s13367-015-0003-2
28. Wei M, Sun L, Qi P, Chang C, Zhu C (2018) Continuous phenomenological modeling for the viscosity of shear thickening fluids. NanomaterNanotechnol 8:184798041878655. https://doi.org/10.1177/1847980418786551
29. Gürgen S, Sofuoğlu MA, Kuşhan MC (2019) Rheological compatibility of multi-phase shear thickening fluid with a phenomenological model. Smart Mater Struct 28(3):035027. https://doi.org/10.1088/1361-665X/ab018c
30. Yegnanarayana B (2006) Artificial neural networks. Prentice-Hall of India, New Delhi
31. Priddy KL, Keller PE (2005) Artificial neural networks: an introduction. SPIE Press, Bellingham, Wash
32. Gürgen S, Kuşhan MC, Li W (2016) The effect of carbide particle additives on rheology of shear thickening fluids. Korea-AustRheol J 28(2):121–128. https://doi.org/10.1007/s13367-016-0011-x
33. Gürgen S, Li W, Kuşhan MC (2016) The rheology of shear thickening fluids with various ceramic particle additives. Mater Des 104:312–319. https://doi.org/10.1016/j.matdes.2016.05.055
34. Nguyen CT et al (2007) Temperature and particle-size dependent viscosity data for water-based nanofluids–Hysteresis phenomenon. Int J Heat Fluid Flow 28(6):1492–1506. https://doi.org/10.1016/j.ijheatfluidflow.2007.02.004
35. Liu X-Q, Bao R-Y, Wu X-J, Yang W, Xie B-H, Yang M-B (2015) Temperature induced gelation transition of a fumed silica/PEG shear thickening fluid. RSC Adv 5(24):18367–18374. https://doi.org/10.1039/C4RA16261G

Publisher's Note Springer Nature remains neutral with regard to jurisdictional claims in published maps and institutional affiliations.